J Solid State Electrochem (2009) 13:1925–1933
DOI 10.1007/s10008-008-0777-y

ORIGINAL PAPER

Microwave-assisted synthesis of organic–inorganic poly(3,4-ethylenedioxythiophene)/$RuO_2{\cdot}xH_2O$ nanocomposite for supercapacitor

Li Chen · Changzhou Yuan · Bo Gao · Shengyao Chen · Xiaogang Zhang

Received: 16 August 2008 / Revised: 14 December 2008 / Accepted: 17 December 2008 / Published online: 14 January 2009

Abstract An organic–inorganic poly(3,4-ethylenedioxythiophene) (PEDOT)/$RuO_2{\cdot}xH_2O$ nanocomposite (approximately 1 wt.% RuO_2) has been successfully prepared for the first time under microwave irradiation within 5 min with power 900 W via in situ chemical polymerization. The morphology and structure of the resultant material is characterized by transmission electron microscope and Fourier transform infrared. Moreover, the electrochemical properties of the synthesized nanocomposite can be controlled by adjusting the annealing temperature, which is definitely illustrated by cyclic voltammetry, galvanostatic charge–discharge, and electrochemical impedance spectra. Electrochemical data have shown that the PEDOT/$RuO_2{\cdot}xH_2O$ nanocomposite annealed at 150 °C possesses the most favorable charge/discharge ability with a specific capacitance of 153.3 F g^{-1} at a current density of 150 mA g^{-1} and the high efficient utilization of PEDOT at various current densities. Furthermore, such composite has a less capacitance degradation of 23.8% after 1,000 continuous cycles. The improved electrochemical performance are mainly attributed to the large electroactive surface of nanocomposite and the existence of amorphous $RuO_2{\cdot}xH_2O$ particles as well as a synergistic effect of the polymer PEDOT and annealed $RuO_2{\cdot}xH_2O$. Thus, the PEDOT/$RuO_2{\cdot}xH_2O$ nanocomposite annealed at 150 °C can act as a promising electroactive material for supercapacitor application.

Keywords Poly(3 · 4-ethylenedioxythiophene) · $RuO_2{\cdot}xH_2O$ · Microwave-assisted · Nanocomposite

L. Chen · C. Yuan · B. Gao · S. Chen · X. Zhang (✉)
College of Material Science & Engineering,
Nanjing University of Aeronautics and Astronautics,
Nanjing 210016, People's Republic of China
e-mail: azhangxg@163.com

Introduction

Recently, there has been a great deal of interest in the synthesis of nanocomposite by using some simple routes for several applications, such as light emitting diodes, chemical sensors, supercapacitors, fuel cells, and so on [1–5]. In particular, the composite combined conjugated polymers with metal oxides at the "nanoscale" level owns much enhanced charge-storage ability for the application of electrochemical capacitors due to the synergistic effects [6, 7]. Commonly, among all kinds of conjugated polymer, poly(3,4-ethylenedioxythiophene) (PEDOT), a derivative of polythiophene, has been paid more attention [8]. Owing to the moderate band gap, unique structural properties, and reaction mechanism, PEDOT has several advantages, such as high transparency in visible regime, excellent environmental stability, low redox potential, good thermal stability, and high conductivity in doped state either n-type or p-type [9, 10]. In addition, the combination of PEDOT and metal oxides also has been demonstrated to offer the improved electrochemical performance. For example, the intercalated PEDOT/MoO_3 composite has been successfully prepared with the enhanced electrochemical properties for supercapacitor [11]. Moreover, Liu and Lee [12] have reported that the PEDOT/MnO_2 composite with the 1D nanostructure can exhibit extreme excellent capacitive and mechanical properties for energy storage applications.

On the other hand, in order to broaden the scope of this organic–inorganic hybrid material based on the polymer PEDOT and enhance their electrochemical redox behaviors, many families of noble transition metal oxides can be considered. Particularly, hydrous ruthenium oxide ($RuO_2{\cdot}xH_2O$) in either crystalline or amorphous hydrous form has been already recognized as the most promising electrode material for electrochemical capacitor [13, 14]

based on the fact that $RuO_2{\cdot}xH_2O$ with the porous structure may show much better reversible faradic capacitive performance in acidic electrolyte according to the following non-stoichiometric reaction [15].

$$RuO_X(OH)_Y+\delta e^-+\delta H^+ \rightleftarrows RuO_{X-\delta}(OH)_{Y+\delta}. \quad (1)$$

Consequently, they can offer a remarkable specific capacitance value ranging from 720 to 760 F g^{-1} [16]. To date, the combination PEDOT with $RuO_2{\cdot}xH_2O$ can enable the distinct elevation of electrochemical properties compared with the common polymer electrode itself. Hong et al. [17] have demonstrated that the PEDOT/RuO_2 composite electrode has an enhanced capacitance of 420 F g^{-1} by depositing RuO_2 on the conducting polymer PEDOT. Huang et al. [18] have reported that PEDOT–PSS/RuO_2 film can show the enhancement of optical and electrochemical properties because PEDOT–PSS can act as a three-dimensional, random, and electronically conducting template which allows the formation of relatively uniform $RuO_2{\cdot}xH_2O$ particles. Unfortunately, the main obstacle for applications at present is that the cost of noble metal is high, the preparation of the organic–inorganic material often is low yield, and the procedure is time-consuming, involving several steps, some additive and higher energy.

Hence, in this study, the PEDOT/$RuO_2{\cdot}xH_2O$ nanocomposite (the mere approximately 1 wt.% RuO_2) can be largely synthesized by in situ chemical polymerization with the simple microwave-assisted within 5 min under power 900 W. To the best of our knowledge, the fast-growing field of synthesized PEDOT-based nanocomposite with $RuO_2{\cdot}xH_2O$ to enhance the electrochemical performance of materials for supercapacitor using microwave-assisted polymerization has not been explored yet. In addition, the influence of annealing temperature upon the electrochemical performance of the resultant PEDOT/$RuO_2{\cdot}xH_2O$ nanocomposite is also investigated here, and the electrochemcial results have illuminated that the PEDOT/$RuO_2{\cdot}xH_2O$ nanocomposite (the mere presence of approximately 1 wt.% RuO_2) annealed at 150 °C can display the favorable electrochemical properties due to the large electroactive surface, the existence of $RuO_2{\cdot}xH_2O$ particles, and a synergistic effect for the nanocomposite. Consequently, the as-synthesized PEDOT/$RuO_2{\cdot}xH_2O$ nanocomposite can be considered as a promising candidate material for supercapacitor application.

Experimental

Synthesis of PEDOT/$RuO_2{\cdot}xH_2O$ (approximately 1 wt.% RuO_2)

3,4-Ethylenedioxythiophene (EDOT, 99%) and $RuCl_3{\cdot}xH_2O$ solution were both obtained from Aldrich. Ammonium persulfate (APS), sulfuric acid (H_2SO_4), and ethanol were analytical grade and purchased from Shanghai Chemical Reagent. Aqueous solution was prepared with doubly distilled water.

The procedure employed for preparing the PEDOT/$RuO_2{\cdot}xH_2O$ nanocomposite was as follows: in a typical synthesis, 0.75 mL EDOT was dispersed in H_2SO_4 solution (30 mL, 0.2 M), followed by slowly adding 1 mL $RuCl_3{\cdot}xH_2O$ solution (0.01 g/mL). Then, APS was mixed with a magnetic stirring and homogenization was continued for 2 h in order to disperse effectively at room temperature. Subsequently, the above mixture was moved into the XH-100A microwave instrument (Haoxiang, Beijing China) which was equipped with a reflux condenser and conducted for a fixed time (5 min) with adequate power (900 W). The result composite was washed several times with distilled water and alcohol by a centrifugal filtration method and dried at 60 °C overnight under vacuum. Finally, the product (the mere presence of approximately 1 wt.% RuO_2) was annealed in air for 3 h at the different temperatures ranging from 100 °C to 200 °C. For comparison, the pristine PEDOT and pristine $RuO_2{\cdot}xH_2O$ were prepared by the same procedure as described above except that the precursor solution was only monomer EDOT and $RuCl_3{\cdot}xH_2O$ solution, respectively.

Morphology characterization

The morphologies and electron diffraction patterns of the samples were examined by transmission electron microscope (TEM, FEI TECNAI-20). Fourier transform infrared (FT-IR) spectra were recorded with a model 360 Nicolet AVATAR spectrophotometer. Atomic force microscopy (AFM, SPA 300HV, Japan) was used to obtain and reconstruct a 3D image of the surface of the samples.

Electrochemical measurements

The working electrode, containing 5 mg as-prepared active material, 0.6 mg acetylene black, and 0.3 mg polytetrafluoroethylene was mixed well for 15 min. Then, the solvent (alcohol) was dropped into the above mixture and ground to form the coating slurry which was smeared onto the pretreated graphite substrates (area, 1 cm^2). Before the electrochemical test, the prepared electrode was dried in air at 50 °C overnight. Electrochemical characterization was carried out in a conventional three-electrode cell with 0.5 M H_2SO_4 as the electrolyte. The platinum foil and saturated calomel electrode were used as the counter and reference electrode, respectively. All electrochemical measurements were performed by CHI660 electrochemical analyzer system (Chenhua, Shanghai China).

Results and discussion

The morphology characteristics of PEDOT/$RuO_2{\cdot}xH_2O$ (approximately 1 wt.% RuO_2) nanocomposite

Typical TEM photographs for the as-synthesized pristine PEDOT and PEDOT/$RuO_2{\cdot}xH_2O$ nanocomposite are illustrated in Fig. 1a, b, respectively. In addition, TEM photograph for the PEDOT/$RuO_2{\cdot}xH_2O$ nanocomposite annealed at 150 °C is also shown in Fig. 1c. Note in Fig. 1a that pristine PEDOT prepared by microwave irradiation method has a clear and uniformly spherical morphology. However, as can be seen from the TEM of PEDOT/$RuO_2{\cdot}xH_2O$, the nanostructure of spherical particles have been become partially sheet-like due to the incorporation of $RuO_2{\cdot}xH_2O$ into the PEDOT. While

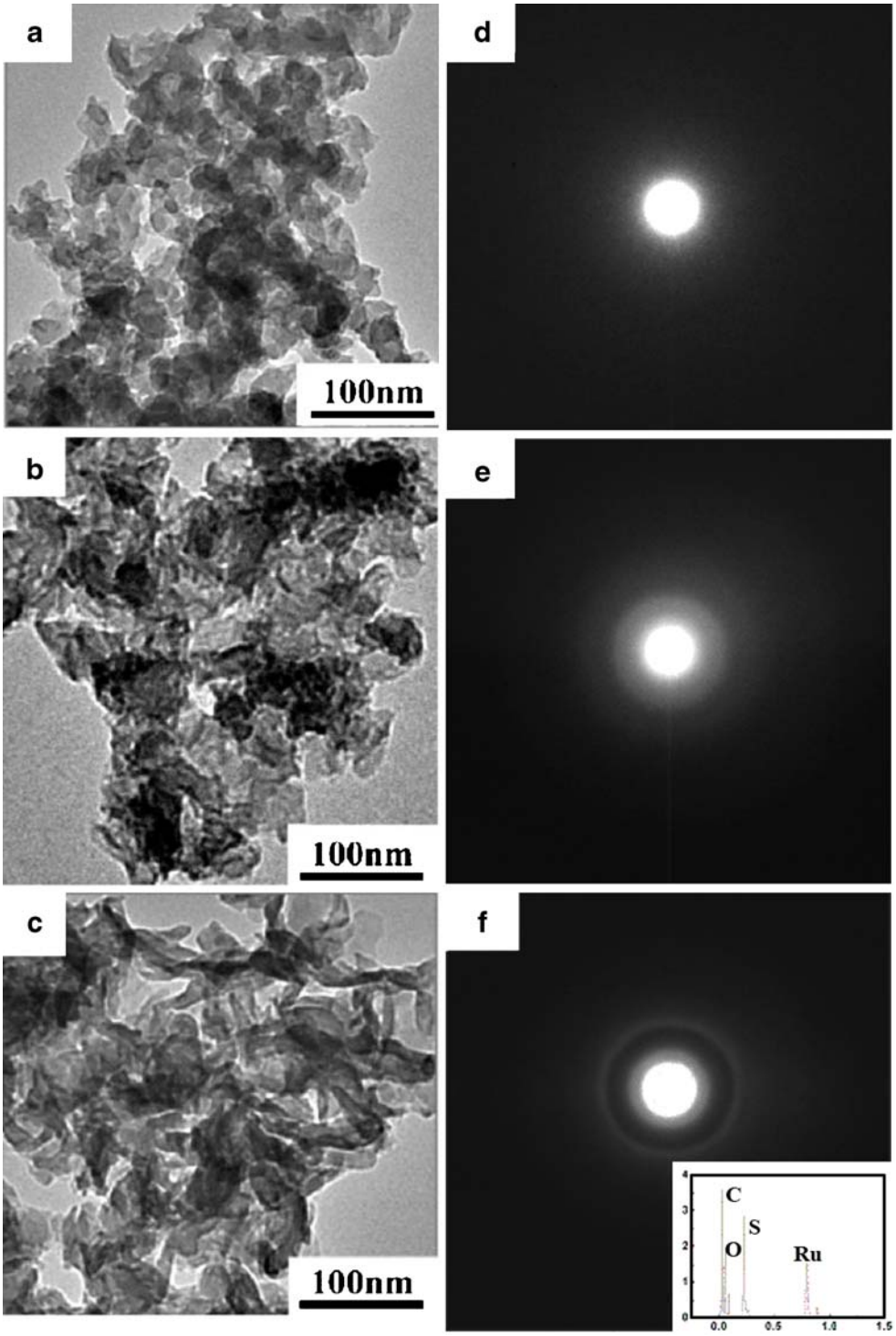

Fig. 1 Typical TEM images and electron diffraction of as-synthesized pristine PEDOT (**a**, **d**), PEDOT/$RuO_2{\cdot}xH_2O$ (with approximately 1 wt.% RuO_2) (**b**, **e**) and the composite annealed at 150 °C (**c**, **f**)

PEDOT/$RuO_2{\cdot}xH_2O$ nanocomposite is further annealed at 150 °C, the TEM image reveals that the sample is assembled by many flake-like particles. Moreover, after a comparison of Fig. 1a–c, the size of pristine PEDOT particles is a little smaller (approximately 20–30 nm) than that of PEDOT/$RuO_2{\cdot}xH_2O$ composite (approximately 35 nm); subsequently, the size ranging from 70 to 80 nm can be found after annealing at 150 °C for the PEDOT/$RuO_2{\cdot}xH_2O$ nanocomposite. The above phenomenon indicates that the morphology and size of the samples should be significantly influenced by the combination with $RuO_2{\cdot}xH_2O$ and the annealing treatment. On the other hand, a comparison of the electron diffraction patterns for as-prepared pristine PEDOT, PEDOT/$RuO_2{\cdot}xH_2O$, and PEDOT/$RuO_2{\cdot}xH_2O$ annealed at 150 °C is shown in Fig. 1d–f. It is apparent that pristine PEDOT is an amorphous structure because of no diffraction rings. However, when PEDOT/$RuO_2{\cdot}xH_2O$ nanoparticle is successfully synthesized and subsequently annealed at 150 °C, the diffraction ring becomes more and more obvious, indicating that $RuO_2{\cdot}xH_2O$ in the nanocomposite system is tardily closer to crystalline with increasing the annealing temperature. Furthermore, the energy dispersive analysis, shown in Fig. 1f, can reveal the existence of Ru, O, C, and S species from the contribution of the nanocomposite composed of PEDOT and $RuO_2{\cdot}xH_2O$.

To further investigate molecular structure of the as-synthesized PEDOT/$RuO_2{\cdot}xH_2O$ nanocomposite by the microwave-assisted method, FT-IR spectra of pristine PEDOT and PEDOT/$RuO_2{\cdot}xH_2O$ nanocomposites annealed at different temperatures are shown as curves a–e in Fig. 2, respectively. Evidently, the curves of PEDOT/$RuO_2{\cdot}xH_2O$ nanocomposite annealed at different temperatures are almost analogical to that of pristine PEDOT until the annealing temperature of the nanocomposite is equal to 180 °C. In curves a–d, it is noted that the vibrations at 1,385 and 1,344 cm^{-1} correspond to the C–C stretching in the thiophene ring, while peaks at 1,156 and 1,093 cm^{-1} are assigned to the stretching modes of the ethylenedioxy group in the molecule. The bands at 984 and 844 cm^{-1} can be ascribed to vibration modes of C–S bond in the thiophene ring. C–S–C stretching appears at 694 cm^{-1}, which is in good accordance with the literature [19]. In addition, the FT-IR spectra also show a small peak at 500 cm^{-1}, which may be influenced by hydrous RuO_2. Nevertheless, the curve of PEDOT/$RuO_2{\cdot}xH_2O$ nanocomposite annealed at 200 °C is completely different from that of the others, which can demonstrate that the nanocomposite is not subjected to further annealing treatment because of the collapse of the PEDOT backbone [20]. The peak at approximately 1,204 cm^{-1} correspond to the O=S=O stretching in molecule of SO_4^{2-}, which can also clearly indicate that H_2SO_4 has been successfully doped into the PEDOT polymer matrix.

Comparative voltammetric behaviors of pristine PEDOT through common chemical process and the microwave irradiation

Figure 3 shows the cyclic voltammograms of the pristine PEDOT electrode from −0.2 to 0.7 V, which is synthesized via common chemical process and the microwave-assisted, respectively. From a comparison of curves a–b, the electrochemical current value of pristine PEDOT prepared by the direct chemical polymerization within 24 h at room temperature is less than that obtained by the rapid microwave process, the reason for which may be that the extreme conditions of microwave method lead to the formation of free radicals, mechanical shocks, high shear gradients, and very rapid and efficient mixing in multiphase systems. Moreover, the microwave effects mentioned above can also explain why the polymerization of PEDOT with higher yield is completed in 5 min, while the common

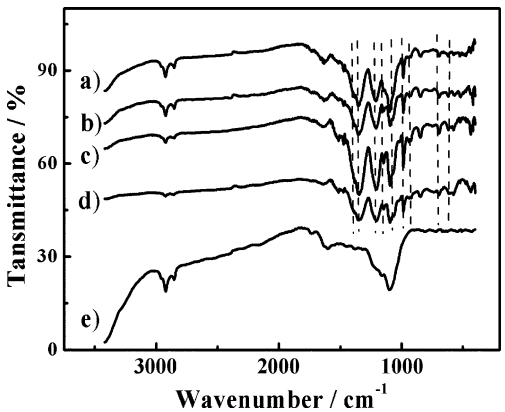

Fig. 2 FT-IR spectra of as-synthesized pristine PEDOT (**a**), PEDOT/$RuO_2{\cdot}xH_2O$ (**b**), and the composite annealed at 150 °C (**c**), 180 °C (**d**), and 200 °C (**e**)

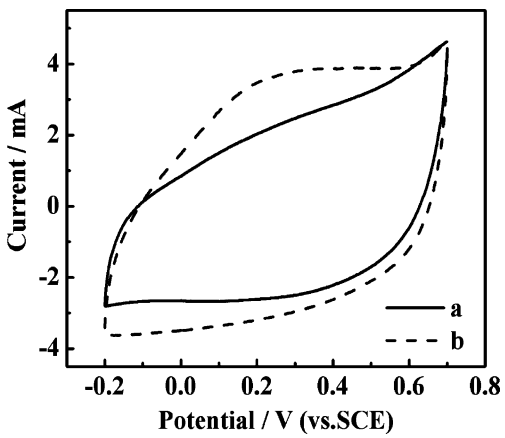

Fig. 3 Cycle voltammograms of the pristine PEDOT via direct chemical polymerization in 24 h (**a**) and microwave process in 5 min (**b**), respectively. Scan rate, 10 mV s^{-1}. Electrolyte, in 0.5 M H_2SO_4

chemically oxidization of PEDOT needs at least 24 h. However, the polymerization process mainly occurs by á–â linking, and the linking is almost impossible to be destroyed easily during polymerization; hence, the microwave irradiation is not likely to change the molecular bonding patterns of PEDOT. The statement is further supported by the FT-IR spectra. Otherwise, because of the high microwave energy, PEDOT chains cannot coagulate with each other, forming the large aggregates consisting of small nucleior or particles, resulting in the formation of spherical particle with the higher porosity as shown in TEM. As a consequence, PEDOT prepared under microwave irradiation has an enhanced current.

Electrochemical behaviors of as-synthesized PEDOT/$RuO_2{\cdot}xH_2O$ (approximately 1 wt.% RuO_2) nanocomposite

The voltammetric behavior of the pristine $RuO_2{\cdot}xH_2O$ electrode with microwave under 900 W for 5 min is also shown as curve 1 in Fig. 4a. In addition, curves 2–4 in Fig. 4a represent the cyclic voltammetric responses of as-prepared pristine $RuO_2{\cdot}xH_2O$ annealed in air for 3 h at 120 °C, 150 °C, and 180 °C, respectively. Obviously, the temperatures at 150 °C is the optimum condition for annealing the pristine $RuO_2{\cdot}xH_2O$ because of the maximal voltammetric current and charge value. In addition, the pristine $RuO_2{\cdot}xH_2O$ annealed at 150 °C also has been demonstrated to have the most ideal capacitive behavior [21]. On the other hand, typical cyclic voltammetry (CV) images measured in 0.5 M H_2SO_4 for as-prepared PEDOT/$RuO_2{\cdot}xH_2O$ and the nanocomposite annealed at 120 °C, 150 °C, and 180 °C are shown as curves 2–5 in Fig. 4b, respectively. In contrast, the CV of as-prepared pristine PEDOT is seen from curve 1 in Fig. 4b. Note that the electrochemical responses of PEDOT/$RuO_2{\cdot}xH_2O$ between the current and the potential approximately follow the same trace of pristine PEDOT, revealing that the addition of approximately 1 wt.% RuO_2 does not significantly increase the total capacitance of the organic–inorganic nanocomposite, although the voltammetric currents of the pristine $RuO_2{\cdot}xH_2O$ is much higher than that of pristine PEDOT based on the CV curves both in Fig. 4a, b. However, the background current value in the potential ranges of −0.2–0.7 V are improved gradually when the annealing temperature increases from 120 °C to 150 °C, indicating that the enhancement of electrochemical performance upon PEDOT incorporation of $RuO_2{\cdot}xH_2O$ could become greatly evident after the annealing treatment. Unfortunately, a drastic decrease of current value is found when the annealing temperature is sequentially raised to 180 °C. The above phenomenon may suggest that the nanocomposite system could reach a maximum of voltammetric charges in the case of annealing at 150 °C. Moreover, from a comparison of curves 2–5, the CV responses between the positive sweep and negative sweep are the most symmetric for curve 4 of the PEDOT/$RuO_2{\cdot}xH_2O$ nanocomposite annealed at 150 °C, suggestive of an ideal electrochemical capacitance property.

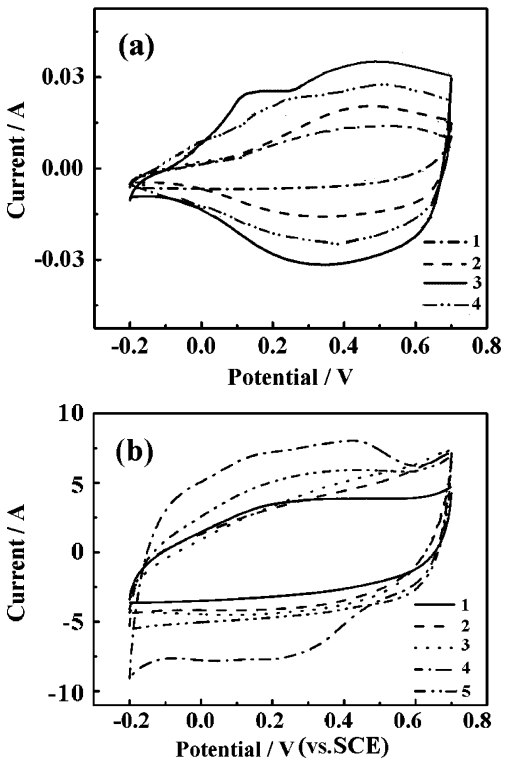

Fig. 4 **a** Cycle voltammograms of as-synthesized pristine $RuO_2{\cdot}xH_2O$ electrode (*1*) and $RuO_2{\cdot}xH_2O$ annealed at 120 °C (*2*), 150 °C (*3*), and 180 °C (*4*). **b** Cycle voltammograms of as-synthesized pristine PEDOT (*1*), PEDOT/$RuO_2{\cdot}xH_2O$ (*2*), and the composite annealed at 120 °C (*3*), 150 °C (*4*)and 180 °C (*5*). Scan rate, 10 mV s^{-1}. Electrolyte, in 0.5 M H_2SO_4

Typical galvanostatic charge–discharge curves measured in a 0.5 M H_2SO_4 solution between −0.2 and 0.7 V at 500 mA g^{-1} for as-prepared pristine PEDOT and PEDOT/$RuO_2{\cdot}xH_2O$ nanocomposite annealed under the different temperatures are shown as curves a–e in Fig. 5, respectively. Clearly, all the charge curves are almost linear and somewhat symmetrical to their discharge counter parts, suggestive of the good electrochemical performance of the samples. The specific capacitance (SC) of the whole working electrode (C_m) can be calculated from the following Eq. 2:

$$C_m = \frac{C}{m} = \frac{I \times t}{\Delta V \times m} \tag{2}$$

where I is the discharge current, t is the overall discharge time, ΔV is the potential range, and m is the mass of

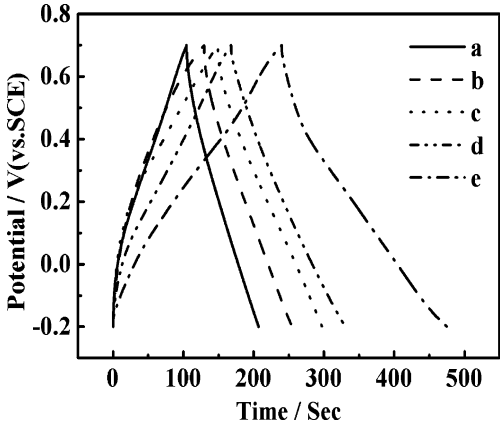

Fig. 5 Charge–discharge behavior of as-synthesized pristine PEDOT (**a**), PEDOT/$RuO_2{\cdot}xH_2O$ (**b**), the composite annealed at 120 °C (**c**), 150 °C (**e**), and 180 °C (**d**) at the current density of 500 mA g^{-1} within a potential window of −0.2–0.7 V. Electrolyte, in 0.5 M H_2SO_4

electroactive material. Based on the curves a–e in Fig. 5, the SC of the electrode can be respectively calculated according to Eq. 2 and listed in Table 1. As a whole, the SC of composite system is higher than that of PEDOT only (55.6 F g^{-1}) due to the pseudocapacitance of $RuO_2{\cdot}xH_2O$ nanoparticles. In addition, it is evident that the absolute SC values of the PEDOT/$RuO_2{\cdot}xH_2O$ nanocomposite system can be enhanced with increasing the annealing temperature and reach a maximum of approximately 132.4 F g^{-1} in the case of annealing at 150 °C, which is in good agreement with the above CV results. The above result can be favored by three points. Firstly, PEDOT/$RuO_2{\cdot}xH_2O$ nanocomposite annealed at 150 °C with the flake-like structure is more accessible to the electrolyte, and more inner electroactive sites for the doping/dedoping process can occur in 3D polymer matrix. The more electroactive surface can be also favored by the AFM analysis in Fig. 6. The AFM analyses clearly indicate that the pristine PEDOT has a homogeneous surface morphology with very low roughness (approximately 0.398 nm). Conversely, the surface morphology of PEDOT/$RuO_2{\cdot}xH_2O$ nanocomposite significantly changes upon the heat treatment at 150 °C. At this stage, coalescence of the nuclei takes place, accompanied by the increase of roughness of the film (approximately 11.4 nm), resulting in the more electroactive surface. Secondly, according to Chen and Hu [22], the electronic conductivity of $RuO_2{\cdot}xH_2O$ commonly may be poor because the amorphous nanostructure should make the electron pathway discontinuous during the charge storage and delivery processes. However, the discontinuity in the electron pathway probably may be improved by the annealing treatment due to the sintering of amorphous $RuO_2{\cdot}xH_2O$; moreover, when amorphous $RuO_2{\cdot}xH_2O$ particles are annealed at 150 °C, the samples may retain the most facile pathways for both electron and proton conduction and have the best utilization of active species, resulting in the considerably high SC. As a consequence, the SC of resultant PEDOT/$RuO_2{\cdot}xH_2O$ nanocomposite is correspondingly promoted. Finally, there may be a synergistic effect for the nanocomposite composed of annealed $RuO_2{\cdot}xH_2O$ and PEDOT.

Table 1 The SC of PEDOT and PEDOT/$RuO_2{\cdot}xH_2O$ composite (with approximately 1 wt.% RuO_2) annealed at different temperatures in 0.5 M H_2SO_4 electrolyte at the current density of 500 mA g^{-1}

Composites		C_m (F g^{-1})
PEDOT (without doped Ru)		55.6
PEDOT/$RuO_2{\cdot}xH_2O$	60	69.1
PEDOT/$RuO_2{\cdot}xH_2O$ annealed at	120	83.5
different temperatures (°C)	150	132.4
	180	89.4

In addition, as seen from Table 1, the SC value of PEDOT/$RuO_2{\cdot}xH_2O$ significantly degrades when the annealing temperature is at 180 °C. The reason could be supported by the fact that the water content of RuO_2 is much less and the crystallization of $RuO_2{\cdot}xH_2O$ has been transformed when further increasing the annealing temperature, which would inhibit the transportation of electrolyte ions in the bulk.

In summary, when the annealing temperature is at 150 °C, the capacitive behavior of as-prepared PEDOT/$RuO_2{\cdot}xH_2O$ nanocomposite is better than that of composite system annealed at any other temperature. Therefore, it would be investigated in detail in the next section. Curves a–d in Fig. 7 show a comparison of the voltammetric behavior for PEDOT/$RuO_2{\cdot}xH_2O$ nanocomposite annealed at 150 °C measured at different scan rates. It is noticeable that all the curves could exhibit the analogously rectangular shape. Meanwhile, the voltammeric charges integrated from the positive sweeps are very close to those integrated from their corresponding negative sweeps, which can illuminate that the electrode has an excellent reversibility. Furthermore, although the scan rate is increasing discontinuously, no obvious distortions in CV curves is observed, indicative of the high power property. All the above results demonstrate that the PEDOT/$RuO_2{\cdot}xH_2O$ nanocomposite annealed at 150 °C can be considered as a potential candidate in the application of electrochemical supercapacitors.

The galvanostatic charge–discharge of as-prepared PEDOT/$RuO_2{\cdot}xH_2O$ nanocomposite annealed at 150 °C measured in 0.5 M H_2SO_4 between −0.2 and 0.7 V under 150, 300, 500, and 800 mA g^{-1} are shown as curves a–d in Fig. 8, respectively. Note that the iR drop turns out to be much obvious with increasing the applied current density.

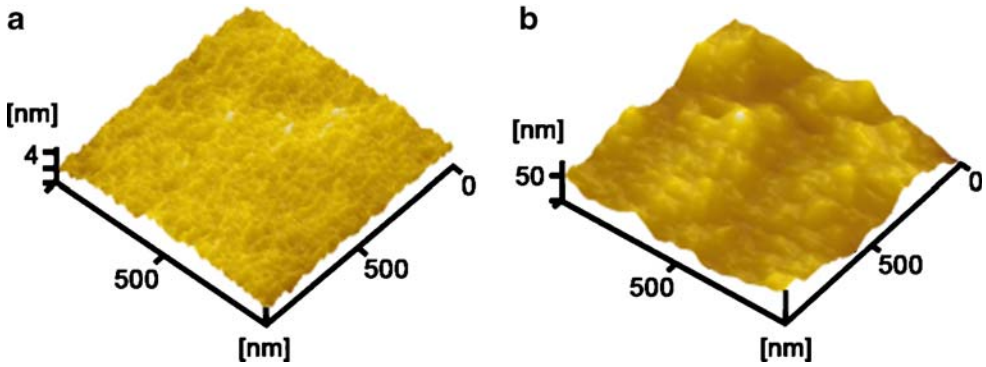

Fig. 6 AFM 3D image for the surface of pristine PEDOT (**a**) and PEDOT/$RuO_2{\cdot}xH_2O$ annealed at 150 °C (**b**)

The effect is likely due to a slight damage of the structure for the PEDOT/$RuO_2{\cdot}xH_2O$ nanocomposite electrode by potentiostatic polarization at a high current density. Fortunately, the charge curves are approximately linear and almost symmetric to the corresponding discharge curves, indicating an ideal capacitor behavior between the electrode and electrolyte. Moreover, the SC of PEDOT/$RuO_2{\cdot}xH_2O$ electrodes discharged from 800- to 150-mA g^{-1} yield can be calculated as Eq. 2. Otherwise, the SC based on the mass of PEDOT in the composite system ($C_{m,PEDOT}$) also can be calculated as Eq. 3:

$$C_{m,PEDOT} = \frac{C_{m,composite} - (1 - w_{PEDOT})C_{m,RuO_2 \cdot xH_2O}}{w_{PEDOT}} \quad (3)$$

where $C_{m,composite}$ is the SC of the composite electrode, $C_{m,RuO_2 \cdot xH_2O}$ is the SC of $RuO_2{\cdot}xH_2O$, w_{PEDOT} is the weight percent of PEDOT in the composite. The total values of the samples are collected and listed in Table 2. As seen from Table 2, the PEDOT/$RuO_2{\cdot}xH_2O$ nanocomposite at a current density of 150 mA g^{-1} has been found to own a SC of approximately 153.3 F g^{-1}, while the SC contributed by the PEDOT in nanocomposite system can reach approximately 149.7 F g^{-1}. Out of question, such high SC may depend on the microstructure of PEDOT/$RuO_2{\cdot}xH_2O$ nanocomposite annealed at 150 °C, which is profitable to more electrolyte active ions intercalation into the bulk material of the PEDOT backbone and $RuO_2{\cdot}xH_2O$ particles. Simultaneously, it is well known that when the current density increases from 150 to 800 mA g^{-1}, the SC loss of about 17% (from 153.3 to127.4 F g^{-1}) for the PEDOT/$RuO_2{\cdot}xH_2O$ nanocomposite can be attributable to the less inner active sites that could be accessed by the electroactive ions to proceed with the redox transition at a higher current density [23]. Table 2 also shows that the SC of PEDOT in the composite system here could be all up to above 120 F g^{-1} at different current densities, suggesting the favorable utilization of PEDOT no matter how high the discharging current density is.

In order to investigate the electrochemical behavior at the electrode/electrolyte interface in detail, electrochemical impedance measurement which used the small sine wave amplitude of 5 mV and broad frequency range of 10^5 to

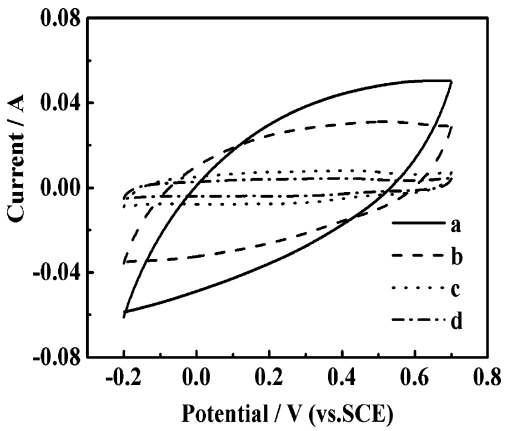

Fig. 7 Cycle voltammograms of as-synthesized PEDOT/$RuO_2{\cdot}xH_2O$ annealed at 150 °C. Scan rates, 100 mV s^{-1} (**a**), 50 mV s^{-1} (**b**), 10 mV s^{-1} (**c**), and 5 mV s^{-1} (**d**). Electrolyte, in 0.5 M H_2SO_4

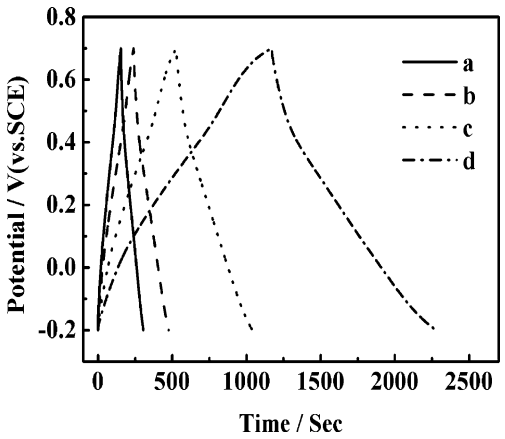

Fig. 8 Charge–discharge behavior of as-synthesized PEDOT/$RuO_2{\cdot}xH_2O$ annealed at 150 °C within a potential window of −0.2–0.7 V. Current densities, 800 mA g^{-1} (**a**), 500 mA g^{-1} (**b**), 300 mA g^{-1} (**c**), and 150 mA g^{-1} (**d**). Electrolyte, in 0.5 M H_2SO_4

Table 2 The SC of PEDOT/$RuO_2{\cdot}xH_2O$ (with approximately 1 wt.% RuO_2) annealed at 150 °C and the SC based on the mass of PEDOT in 0.5 M H_2SO_4 electrolyte at different current densities

Current densities (mA g^{-1})	C_m (F g^{-1})	$C_{m,PEDOT}$ (F g^{-1})
800	127.4	124.4
500	132.4	129.4
300	142.5	139.1
150	153.3	149.7

10^{-2} Hz is carried out at open-circuit potentials in 0.5 M H_2SO_4 electrolyte. Complex plane plots of the impedance of PEDOT/$RuO_2{\cdot}xH_2O$ nanocomposite annealed at 150 °C and pristine PEDOT electrodes via microwave process are presented in Fig. 9, respectively. As shown in the inset, it is obvious that the nanocomposite has the smaller radius of semicircle in high-frequency region after the introduction of $RuO_2{\cdot}xH_2O$. Furthermore, the charge transfer resistance (R_{ct}) related to the faradic process of electrodes can be estimated according to the radius of semicircle; hence, the nanocomposite electrode is demonstrated to have the lower R_{ct} of 0.5 Ω dropping from 0.8 Ω of pristine PEDOT, which should be ascribed to the more ion intercalation, emersion, and, subsequently, the increase of the effective active sites for faradic reactions. As a consequence, the PEDOT/$RuO_2{\cdot}xH_2O$ nanocomposite annealed at 150 °C has a significant improvement on the conductivity in comparison with the pristine PEDOT. In the low-frequency region, the imaginary part of curve b is more vertical with the real part than that of curve a, which can clearly present the more excellent ideal capacitive behavior of the annealed nanocomposite.

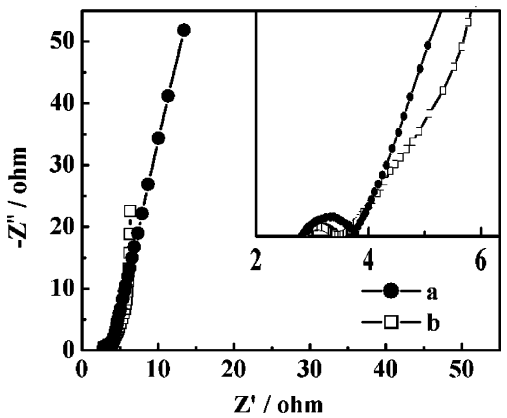

Fig. 9 Typical complex plane impedance plots for as-synthesized pristine PEDOT (**a**), PEDOT/$RuO_2{\cdot}xH_2O$ annealed at 150 °C (**b**) measured at open-circuit potential. *Inset*, data in the high-frequency region. Electrolyte, in 0.5 M H_2SO_4

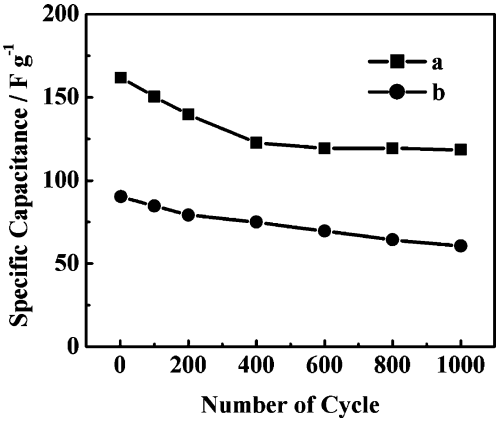

Fig. 10 Cycle life of as-synthesized PEDOT/$RuO_2{\cdot}xH_2O$ annealed at 150 °C (**a**), the pristine PEDOT gained from microwave-assisted (**b**). Electrolyte, in 0.5 M H_2SO_4

In order to test the cycle life of the nanocomposite, the SC against the CV cycle number in 0.5 M H_2SO_4 for the pure PEDOT and the PEDOT/$RuO_2{\cdot}xH_2O$ nanocomposite annealed at 150 °C are shown in Fig. 10. From curves a–b, the electrochemical stability of the nanocomposite electrode is higher than that of the pristine PEDOT in the whole 1,000 cycles. Importantly, a rapid loss in capacitance for the PEDOT/$RuO_2{\cdot}xH_2O$ nanocomposite electrode is clearly found during the initial 400 cycles (from approximately 160 to approximately 125 F g^{-1}), while the SC loss becomes negligible when the cycle number of CV is above 400. Therefore, though the recyclability of hydrous RuO_2 is poor in H_2SO_4 solution, the SC of nanocomposite system is only decayed out approximately 23.8%, while the loss of SC for the pristine PEDOT is up to approximately 33.3% during the whole consecutive cycle. Consequently, the cycle stability of the organic–inorganic hybrid PEDOT/$RuO_2{\cdot}xH_2O$ nanocomposite annealed at 150 °C is even better than that of pristine PEDOT electrode.

Conclusions

In conclusion, PEDOT/$RuO_2{\cdot}xH_2O$ nanocomposite (the mere presence of approximately 1 wt.% RuO_2) have been successfully prepared via the one-step microwave-assisted method, which is simple, easy, efficient, and environmentally friendly. The relationships between the annealing conditions and structural changes for the resultant materials have been investigated based on the TEM and FT-IR data. In addition, the CV, galvanostatic charge–discharge, and electrochemical impedance spectra have demonstrated that the organic–inorganic hybrid PEDOT/$RuO_2{\cdot}xH_2O$ nanocomposite annealed at 150 °C possess the best electrochemical properties in three-electrode cell system,

highlighting the SC of 153.3 F g^{-1} at a current density of 150 mA g^{-1}, the high efficient utilization of PEDOT in the nanocomposite system at various current densities, and a capacitance degradation of 23.8% after 1,000 continuous cycles. Here, the improvement of electrochemical performance could be mainly attributed to the large electroactive surface of nanocomposite for faradic reaction, the existence of amorphous $RuO_2{\cdot}xH_2O$ particles at 150 °C, and a synergistic effect of the polymer PEDOT and the annealed $RuO_2{\cdot}xH_2O$. Therefore, all of above suggest that the PEDOT/$RuO_2{\cdot}xH_2O$ nanocomposite annealed at 150 °C is a very promising supercapacitor electrode material. Furthermore, the microwave-assisted method described here could be further developed to be versatile for the synthesis of other kinds of polymer-based materials.

Acknowledgements This work was supported by National Basic Research Program of China (973 Program no. 2007CB209703) and National Natural Science Foundation of China (nos. 20633040, 20873064), Graduate Innovation Plan of Jiangsu Province (CX07B-089Z).

Reference

1. Colvin VL, Schlamp MC, Alivisatos AP (1994) Nature 370:354. doi:10.1038/370354a0
2. Arbizzani C, Mastragostino M, Meneghello L, Paraventi R (1996) Adv Mater 8:331. doi:10.1002/adma.19960080409
3. Baraton MI, Merhara L, Wang J, Gonsalves KE (1998) Nanotechnology 9:356. doi:10.1088/0957-4484/9/4/010
4. Rajesh B, Thambi KR, Bonard JM, Xanthapolous N, Mathieu HJ, Viswanathan B (2002) Electrochem Solid-State Lett 5:E71. doi:10.1149/1.1518610
5. Mattes BR, Knobbe ET, Fuqua PD, Nishid F, Chang EW, Pierce BM, Dunn B, Karner RB (1991) Synth Met 43:3183. doi:10.1016/0379-6779(91)91262-9
6. Rios EC, Rosario AV, Mello RM, Micaroni L (2007) J Power Sources 163:1137. doi:10.1016/j.jpowsour.2006.09.056
7. Zhang L, Wang M (2003) J Phys Chem B 107:6748. doi:10.1021/jp034130g
8. Zhang X, Lee JS, Lee GS, Cha DK, Moon JK, Yang DJ, Manohar SK (2006) Macromolecules 39:470. doi:10.1021/ma051975c
9. Gustafsson JC, Liedberg B, Inganas O (1994) Solid State Ion 69:145. doi:10.1016/0167-2738(94)90403-0
10. Chiu WW, Sejdic JT, Cooney RP, Bowmaker GA (2005) Synth Met 155:80. doi:10.1016/j.synthmet.2005.06.012
11. Muruganand AV, Viswanath AK (2006) J Appl Phys 100:074319. doi:10.1063/1.2356788
12. Liu R, Lee SB (2008) J Am Chem Soc 130:2942. doi:10.1021/ja7112382
13. Wang YG, Zhang XG (2004) Electrochim Acta 49:1957. doi:10.1016/j.electacta.2003.12.023
14. Panic V, Vidakovic T, Gojkovic S, Dekanski A, Milonjic S, Nikolic B (2003) Electrochim Acta 48:3805. doi:10.1016/S0013-4686(03)00514-0
15. Trasatti S, Kurzweil P (1994) Platin Met Rev 46:38
16. Fang QL, Evans DA, Roberson SL, Zheng JP (2001) J Electrochem Soc 148:A833. doi:10.1149/1.1379739
17. Hong JI, Yeo IH, Paika WK (2001) J Electrochem Soc 148:A156. doi:10.1149/1.1342166
18. Huang LM, Wen TC, Gopalan A (2006) Electrochim Acta 51:3469. doi:10.1016/j.electacta.2005.09.049
19. Han DX, Yang GF, Niu L, Ivaska A (2007) J Electroanal Chem 602:24. doi:10.1016/j.jelechem.2006.11.027
20. Wang JC, Yu XF, Li YX, Liu Q (2007) J Phys Chem C 111:18073. doi:10.1021/jp0749468
21. Hu CC, Liu MJ, Chang KH (2007) J Power Sources 163:1126. doi:10.1016/j.jpowsour.2006.09.060
22. Chen WC, Hu CC (2004) J Power Sources 125:292. doi:10.1016/j.jpowsour.2003.08.001
23. Liang YY, Li HL, Zhang XG (2007) J Power Sources 173:599. doi:10.1016/j.jpowsour.2007.08.010